

Analysis and Deperturbation of the  $C^2\Pi$  and  $D^2\Sigma^+$  States of CaFC. M. GITTINS,\* N. A. HARRIS,\* R. W. FIELD,\* J. VERGÈS,† C. EFFANTIN,‡  
A. BERNARD,‡ J. D'INCAN,‡ W. E. ERNST,§ P. BÜNDGEN,||<sup>1</sup> AND B. ENGELS||\* *Department of Chemistry, M.I.T., Cambridge, Massachusetts 02139; † Laboratoire Aimé-Cotton, C.N.R.S. II, 91405 Orsay Cedex, France; ‡ Laboratoire de Spectrométrie Ionique et Moléculaire, C.N.R.S. et Université Claude-Bernard, 69622 Villeurbanne Cedex, France; § Department of Physics, Davey Laboratory, The Pennsylvania State University, University Park, Pennsylvania 16802; and || Institut für Physikalische und Theoretische Chemie, Universität Bonn, Wegelerstraße 12, 53 Bonn 1, Germany*

The  $C^2\Pi$  and  $D^2\Sigma^+$  states of CaF have been investigated using three different laser-based techniques: laser excited Fourier transform-dispersed fluorescence, optical-optical double resonance, and fluorescence excitation spectroscopy. A perturbation between  $C^2\Pi$ ,  $v = 0$  and  $D^2\Sigma^+$ ,  $v = 0$  has been observed and analyzed. Molecular constants are reported for the  $C$  and  $D$  states.

Main Constants (in  $\text{cm}^{-1}$ )<sup>a</sup>

	$C^2\Pi$	$D^2\Sigma^+$
$T_e$	30269.21(15)	30124.33(7)
$\omega_e$	481.78(40)	657.33(15)
$\omega_e x_e$	1.95(6)	2.85(2)
$B_e$	0.32439(1)	0.3656(2)
$\alpha_e$	0.00205(2)	0.0021(4)

<sup>a</sup> Uncertainties in parentheses are  $2\sigma$ .

© 1993 Academic Press, Inc.

## 1. INTRODUCTION

The alkaline earth monohalides ( $MX$ ) are well described as simple three-particle systems consisting of two closed shell atomic ions ( $M^{2+}$ ,  $X^-$ ) and a single electron. All observed electronic transitions in the  $MX$  molecules correspond to excitation of the unpaired electron from one nonbonding, metal-centered orbital to another. Because of the simplicity of their composition,  $MX$  molecules serve as the archetype for the structure and electron-nuclei energy exchange processes of more complex dipolar core molecules.

This investigation of the  $D^2\Sigma^+$  and  $C^2\Pi$  states of calcium monofluoride (CaF) lies at the intersection of what might be referred to as "top-down" and "bottom-up" approaches to the interpretation of the  $MX$  electronic structure. The bottom-up approach extends the methodology used to understand the CaF valence states, e.g., Crystal Field Theory, to states of higher energy (Rydberg states). The top-down approach seeks to extend models relevant to highly excited electronic states, e.g., Multichannel

<sup>1</sup> Present address: University of New Brunswick, Department of Chemistry, Fredericton, New Brunswick, Canada E3B 6E2.

Quantum Defect Theory, to lower energy. Detailed discussions of the CaF electronic structure may be found elsewhere (1-9).

The  $D^2\Sigma^+$  state was originally observed by Fowler in 1941 (10). It was assumed in his analysis that the lowest observed vibrational level was  $v = 0$ ; however, it is now clear that Fowler observed  $1 \leq v \leq 13$ , not  $0 \leq v \leq 12$ . Bernath observed  $v = 0$  of the  $D$  state over 10 years ago (8) but, misled by Fowler's incorrect assignment, identified it as  $v = 0$  of a separate electronic state and named the state  $C'^2\Sigma^+$ . Experimental observations now show that there is only one  $^2\Sigma^+$  state of CaF in the region between 19 000 and 34 000  $\text{cm}^{-1}$ . This conclusion is supported by the ab initio calculations of Bündgen *et al.* (9).

It has been demonstrated that each core-penetrating Rydberg series of CaF may be extrapolated back to a valence state precursor (2) and that scaling relations meaningful for Rydberg states retain their predictive power from high energy all the way down to the valence region (3). Murphy *et al.*'s (2) extrapolation of Rydberg series was based on the quantum defect calculated for each electronic state. (The quantum defect should remain constant within a Rydberg series.) This method of categorization, combined with a mistaken belief in the existence of both  $C'^2\Sigma^+$  and  $D^2\Sigma^+$  states, led to the suggestion that the lowest energy  $'p'\Sigma$  Rydberg orbital was drastically reshaped because of the increased probability of finding the electron in the molecular ion core (2). The effect of the long-standing  $C' \sim D$  misconception on the interpretation of the  $'s'\Sigma$  Rydberg series was also noticeable, but not nearly as dramatic as for the  $'p'\Sigma$  series. Our recent observations show that both the  $'s'\Sigma$  and  $'p'\Sigma$  Rydberg series extrapolate smoothly to low energy.

We have also observed and analyzed a perturbation between the  $v = 0$  levels of the  $C$  and  $D$  states. The  $D^2\Sigma^+$  and  $C^2\Pi$  states are coupled through the spin-orbit and L-uncoupling operators in the molecular Hamiltonian. We present an analysis of the perturbation using a standard  $^2\Sigma^+(\sigma) \sim ^2\Pi(\pi)$  Hamiltonian (11).

## 2. EXPERIMENTAL DETAILS

The  $C \sim D$  state analysis involves three types of data:  $C-X$  fluorescence excitation spectra,  $D-A$ ,  $D-B$ , and  $C-B$  Fourier transform-dispersed fluorescence spectra, and optical-optical double resonance (OODR) spectra.

$C-X$  laser excitation spectra between 30 190 and 30 232  $\text{cm}^{-1}$  were recorded at the Freie Universität Berlin. A collimated CaF molecular beam was crossed by a beam of tunable single mode UV laser light from a Coherent 699-21 ring dye laser with an intracavity frequency doubler yielding sub-Doppler resolution with a 0.001  $\text{cm}^{-1}$  linewidth.  $C^2\Pi_{1/2}-X^2\Sigma^+(0, 0)$  and  $C^2\Pi_{3/2}-X^2\Sigma^+(0, 0)$  subbands were assigned to rotational quantum numbers up to  $J'' = 27.5$  and 38.5, respectively, and absolute wavenumbers were determined with 0.01  $\text{cm}^{-1}$  accuracy. Details are described in Ref. (12).

$D-A$ ,  $D-B$ , and  $C-B$  induced fluorescence spectra were recorded at the Laboratoire Aimé Cotton. Spectra were obtained following excitation by the UV  $\text{Kr}^{2+}$  laser line at 29 261  $\text{cm}^{-1}$ . They were recorded at a resolution corresponding to a linewidth of 0.030  $\text{cm}^{-1}$  by Fourier transform spectrometry.

The OODR spectra were recorded at MIT for low  $J$ 's of  $v = 0$  and  $v = 1$  of the  $D$  state and in the region of the  $C^2\Pi_{3/2}$ ,  $v = 0 \sim D^2\Sigma^+$ ,  $v = 0$  avoided crossing ( $J \sim 46.5$ ). Low  $J$  spectra were obtained using CaF generated in a laser ablation-supersonic molecular beam apparatus and were recorded at an accuracy of  $\pm 0.03 \text{ cm}^{-1}$ . The rotational temperature in the jet ( $\sim 25 \text{ K}$ ) precluded the observation of levels with  $J > 9.5$ . The  $C^2\Pi_{3/2} \sim D^2\Sigma^+$  avoided crossing data were obtained using the same high

temperature oven in which Murphy *et al.* (2) recorded CaF Rydberg state spectra. Lines near the avoided crossing were recorded to  $\pm 0.10 \text{ cm}^{-1}$ .

The OODR experiment involved two Nd:YAG (Spectra Physics DCR series) pumped pulsed dye lasers. One dye laser (Quanta Ray PDL-1) is tuned to an assigned transition in the  $A^2\Pi_{3/2}-X^2\Sigma^+(0,0)$  band, and the tunable output from a second dye laser (Lumonics HD-300 or Lambda Physik FL3002E), delayed  $\sim 5$  nsec relative to the first, is scanned through  $D-A$  transitions. Transitions into the  $D$  state were detected by monitoring ultraviolet  $D-X$  fluorescence through a 303- to 340-nm transmitting interference filter. By populating a single  $J$ ,  $e/f$  parity level in the intermediate state, the OODR spectrum is reduced to a pattern consisting of two, three, or four lines. This allows for rapid determination of the rotational and spin-rotation constants. A discussion of the two, three, and four line patterns present in the OODR spectra of CaF may be found in Ref. (2).

### 3. ANALYSIS

Rotational analyses of the  $C^2\Pi$  state have been performed by Ernst *et al.* (12) and Vergès *et al.* (13); however, neither group explicitly accounted for the  $C \sim D$  perturbation. In the present paper, spectroscopic constants for the  $C$  and  $D$  states were determined by a nonlinear least-squares fit of observed  $C-X$ ,  $C-B$ ,  $D-A$ , and  $D-B$  transitions to standard  $^2\Pi$  and  $^2\Sigma^+$  energy level expressions. All  $C-X$  fluorescence excitation lines used in the present spectral fit have been previously published in Ref. (12). We have assigned 14 lines from Ernst *et al.*'s (12) Table II, column c, to the  $R_1$  branch of the  $C^2\Pi-X^2\Sigma^+(0,0)$  band. The  $X$ ,  $A$ , and  $B$  state molecular constants have been determined previously (14-16). The elements of the  $3 \times 3$  matrix used to describe the  $C \sim D$  interaction are well known (11). They are reproduced in Table I for clarity. The fitted values of the Hamiltonian parameters are summarized in Table II.

Although the  $T_v$ ,  $A_v$ , and  $B_v$  constants of the  $C$  and  $D$  states remain essentially unchanged when derived from global rather than single electronic state fits, the  $\Lambda$ -

TABLE I  
Hamiltonian Matrix for a  $^2\Pi(\pi) \sim ^2\Sigma^+(\sigma)$  Interaction<sup>a</sup>

$^2\Pi_{3/2}$	$^2\Pi_{1/2}$	$^2\Sigma^+_{1/2}$
$T_{\Pi} + \frac{1}{2}A_{\Pi}$ $+ (B_{\Pi} + A_{\Pi})(x^2 - 2)$ $+ D_{\Pi}[1 - x^2 - (x^2 - 2)^2]$ $+ \frac{1}{2}q(x^2 - 1)$	$-(B_{\Pi} + \frac{1}{4}p)(x^2 - 1)^{1/2}$ $+ 2D_{\Pi}(x^2 - 1)^{3/2}$ $- \frac{1}{2}q(1 \mp x)(x^2 - 1)^{1/2}$	$-\beta(x^2 - 1)^{1/2}$
sym.	$T_{\Pi} - \frac{1}{2}A_{\Pi} + (B_{\Pi} - A_{\Pi})x^2$ $+ D_{\Pi}(1 - x^2 - x^4)$ $+ \frac{1}{2}p(1 \mp x) + \frac{1}{2}q(1 \mp x)^2$	$\alpha + \beta(1 \mp x)$
sym.	sym.	$T_{\Sigma} + B_{\Sigma}x(x \mp 1)$ $- D_{\Sigma}x^2(x \mp 1)^2$ $- \frac{1}{2}r(1 \mp x)$

$$x = J + \frac{1}{2}$$

<sup>a</sup> Matrix elements are calculated using an  $e/f$  parity basis and are written e over f.

TABLE II  
Best-Fit Values of Hamiltonian Parameters (in  $\text{cm}^{-1}$ )<sup>a</sup>

parameter	$C^2\Pi, v=0$	$D^2\Sigma^+, v=0$
T <sup>b</sup>	30215.949(2)	30158.617(2)
A	29.320(4)	
B	0.323368(8)	0.36544(1)
$10^4 A_D$	0.95(5)	
$10^7 D$	5.84(5)	4.5(1)
$10^3 p/\gamma$	1.1(2)	0.3(2)
$10^4 q$	-1.08(4)	
$\alpha$		-1.562(7)
$\beta$		0.0600(2)

<sup>a</sup> Uncertainties in parentheses represent two standard deviations.

<sup>b</sup> The  $v=0, N=0$  level of the  $X^2\Sigma^+$  state is defined as the zero of energy.

doubling and spin-rotation constants change significantly. The perturbation parameter  $\alpha$  is the  ${}^2\Pi \sim {}^2\Sigma$  off-diagonal spin-orbit matrix element multiplied by the  $v_{11} \sim v_{22}$  vibrational overlap factor.

$$\alpha \equiv \langle C^2\Pi | \hat{A}L \cdot S | D^2\Sigma^+ \rangle \langle v_C | v_D \rangle. \quad (1)$$

The molecular spin-orbit operator can be written as a one-electron operator acting on the unpaired,  $\text{Ca}^+$  centered electron,

$$H^{\text{so}} = \hat{A}L \cdot S = \hat{a}[l_z s_z + \frac{1}{2}(l_+ s_- + l_- s_+)] \quad (2)$$

$$\alpha \equiv \langle C^2\Pi | \hat{A}L \cdot S | D^2\Sigma^+ \rangle \langle v_C | v_D \rangle = \frac{1}{2} \langle \pi | \hat{a}l_+ | \sigma \rangle \langle v_C | v_D \rangle \quad (3)$$

$$\alpha(\text{fit}) = -1.562(7) \text{ cm}^{-1}.$$

The vibrational overlap factor,  $\langle v_C = 0 | v_D = 0 \rangle$ , is calculated using an RKR-FCF program descended from a program written by Zare and Cashion (17).

$$\langle v_C = 0 | v_D = 0 \rangle = 0.48_1 \quad (4)$$

$$a_{CD} \equiv \langle C^2\Pi | \hat{A}L \cdot S | D^2\Sigma^+ \rangle = \frac{1}{2} \langle \pi | \hat{a}l_+ | \sigma \rangle = -3.2_5 \text{ cm}^{-1}. \quad (5)$$

The  $C$  and  $D$  state wavefunctions are also mixed by the rotational portion of the molecular Hamiltonian, specifically by the  $L$ -uncoupling operator,

$$\langle {}^2\Pi, v_{11} | H^{\text{rot}} | {}^2\Sigma^+, v_{22} \rangle = \langle {}^2\Pi, v_{11} | -\hat{B}(J^+ L^- + J^- L^+) | {}^2\Sigma^+, v_{22} \rangle. \quad (6)$$

Because  $\text{CaF}$  is effectively a one-electron system, the molecular  $L$ -uncoupling operator,  $L^\pm$ , reduces to a one-electron operator,  $l^\pm$ . The off-diagonal  $C \sim D$  matrix elements are calculated using an  $e/f$  parity basis. The  $\mp$  sign corresponds to  $e/f$  parity.

$$\langle {}^2\Pi_{1/2}, v_{11} | H^{\text{rot}} | {}^2\Sigma^+, v_{22} \rangle = \langle {}^2\Pi(\pi), v_{11} | \hat{B}l^+ | {}^2\Sigma^+(\sigma), v_{22} \rangle [1 \mp (J + \frac{1}{2})] \quad (7)$$

$$\langle {}^2\Pi_{3/2}, v_{11} | H^{\text{rot}} | {}^2\Sigma^+, v_{22} \rangle$$

$$= -\langle {}^2\Pi(\pi), v_{11} | \hat{B}l^+ | {}^2\Sigma^+(\sigma), v_{22} \rangle [(J - \frac{1}{2})(J + \frac{3}{2})]^{1/2}. \quad (8)$$

Equations (7) and (8) may be further simplified to

$$\langle {}^2\Pi(\pi), v_{\Pi} | \hat{B}l^+ | {}^2\Sigma^+(\sigma), v_{\Sigma} \rangle = \langle {}^2\Pi(\pi) | l^+ | {}^2\Sigma^+(\sigma) \rangle \langle v_{\Pi} | \hat{B} | v_{\Sigma} \rangle = b B_{v_{\Pi}v_{\Sigma}}. \quad (9)$$

The off-diagonal rotational constant,  $\langle v_{\Pi} | \hat{B} | v_{\Sigma} \rangle$ , may be calculated using our RKR-FCF program. The matrix element,  $b$ , between electronic wavefunctions resulting from the L-uncoupling operator can in principle be calculated from the knowledge of atomic  $n/\lambda$  parentage of the CaF molecular wavefunctions. In practice however, accurate calculation of  $b$  is nontrivial, as the calculation requires taking the derivative of the electronic wavefunction. We have determined the value of  $b$  from the fit parameter  $\beta$  and the calculated value of  $B_{v_{\Pi}v_{\Sigma}}$ .

$$\beta(\text{fit}) = b B_{v_{\Pi}v_{\Sigma}} \equiv \langle {}^2\Pi(\pi), v_{\Pi} | \hat{B}l^+ | {}^2\Sigma^+(\sigma), v_{\Sigma} \rangle = 0.0600(2) \text{ cm}^{-1} \quad (10)$$

$$B_{0,0}(\text{calc}) \equiv \left\langle v_C = 0 \left| \frac{1}{2\mu R^2} \right| v_D = 0 \right\rangle = 0.16_6 \text{ cm}^{-1} \quad (11)$$

$$b = \frac{\beta(\text{fit})}{B_{0,0}(\text{calc})} = 0.36_1. \quad (12)$$

The  $a_{CD}$  and  $b$  parameters will be used to calculate the contribution of the  $C \sim D$  unique perturber pair to the  $C$  and  $D$  state  $\Lambda$ -doubling and spin-rotation constants.

The  $\Lambda$ -doubling and spin-rotation constants determined by the global fit to  $J \leq 50.5$  levels reflect only the effects of remote vibronic states. The splitting of  $e$  and  $f$  parity levels is determined primarily by the  $\langle C^2\Pi, v = 0 | H^{\text{so}} + H^{\text{rot}} | D^2\Sigma^+, v = 0 \rangle$  matrix elements. When the  $\Lambda$ -doubling constants are determined from separate, low- $J$ -only fits, the off-diagonal matrix elements are folded into the fitted constants (Van Vleck transformation). The relation between  $\Lambda$ -doubling constants and  ${}^2\Pi \sim {}^2\Sigma^+$  off-diagonal matrix elements is described in Lefebvre-Brion and Field (18).

The  $\Lambda$ -doubling and spin-rotation constants determined from the low  $J$  fits of Vergès *et al.* (13) are in good agreement with the values calculated using the constants from the  $3 \times 3$  global fit.

$$\begin{aligned} p_{\text{fit,Ref.(13)}} &= -0.0085(4) \text{ cm}^{-1} \\ &\cong \frac{4\alpha\beta}{E_{11,1/2} - E_{\Sigma}} + p_{\text{fit},3 \times 3} = -0.0077(3) \text{ cm}^{-1} \end{aligned} \quad (13)$$

$$\begin{aligned} \gamma_{\text{fit,Ref.(13)}} &= -0.0090(3) \text{ cm}^{-1} \\ &\cong \frac{4\alpha\beta}{E_{11,1/2} - E_{\Sigma}} + \gamma_{\text{fit},3 \times 3} = -0.0085(2) \text{ cm}^{-1}. \end{aligned} \quad (14)$$

(Uncertainties in parentheses are  $2\sigma$ .)

The  $p$ ,  $q$ , and  $\gamma$  constants can be partitioned into contributions from the  $C \sim D$  interaction and contributions from remote  ${}^2\Pi$  and  ${}^2\Sigma^+$  states. The contributions to  $p$ ,  $q$ , and  $\gamma$  from the  $C, v = 0 \sim D, v > 0$  and  $D, v = 0 \sim C, v > 0$  interactions (denoted  $p_{\text{calc}}$ ,  $q_{\text{calc}}$ , and  $\gamma_{\text{calc}}$ ) are calculated below. Vibrational matrix elements are calculated using the aforementioned RKR-FCF program.

$$\begin{aligned} p_{\text{calc}} &= 4a_{CD}b \sum_{v_D > 0} \frac{\langle v_C = 0 | v_D \rangle \left\langle v_C = 0 \left| \frac{1}{2\mu R^2} \right| v_D \right\rangle}{E_{v_C} - E_{v_D}} = +0.0013 \text{ cm}^{-1} \\ p_{\text{fit},3 \times 3} &= +0.0011(2) \text{ cm}^{-1}. \end{aligned} \quad (15)$$

The values of  $p_{\text{calc}}$  and  $p_{\text{fit},3 \times 3}$  are the same to within the uncertainty of our calculations. We conclude that the contributions to  $p_{\text{fit},3 \times 3}$  from remote  ${}^2\Sigma^+$  states sum to a negligible value.

A similar determination of  $q_{\text{calc}}$  shows that  $v > 0$  levels of the  $D$  state contribute very little to the value of  $q_{\text{fit}}$ .

$$q_{\text{calc}} = 2b^2 \sum_{v_D > 0} \frac{\left| \left\langle v_C = 0 \left| \frac{1}{2\mu R^2} \right| v_D \right\rangle \right|^2}{E_{v_C} - E_{v_D}} = -0.2 \times 10^{-4} \text{ cm}^{-1} \quad (16)$$

$$q_{\text{fit},3 \times 3} = -1.08(4) \times 10^{-4} \text{ cm}^{-1}.$$

We had anticipated that  $q_{\text{fit},3 \times 3}$  would be nearly identical to  $q_{\text{calc}}$ . We find, however, that  $D^2\Sigma^+$ ,  $v > 0$  levels account for only  $\sim 20\%$  of the value of  $q_{\text{fit}}$ . The conclusion we draw is that higher energy  ${}^2\Sigma^+$  states, in particular the  $E^2\Sigma^+$  state, the second member of the ' $d'$ '  $\Sigma$  Rydberg series, make a nonnegligible contribution to the  $\Lambda$ -doubling of the  $C^2\Pi$  state. Presumably this contribution is not reflected in the  $p$  parameter because the value of  $a_{CE}$ , analogous to  $a_{CD}$  in Eqs. (5) and (15), is quite small.

Similarly, the  $D$  state spin-rotation splitting does not appear to be due solely to the  $C$  state.

$$\gamma_{\text{calc}} = 4a_{CD}b \sum_{v_C > 0} \frac{\langle v_D = 0 | v_C \rangle \langle v_D = 0 | \frac{1}{2\mu R^2} | v_C \rangle}{E_{v_C} - E_{v_D}} = -0.0017 \text{ cm}^{-1} \quad (17)$$

$$\gamma_{\text{fit},3 \times 3} = +0.0003(2) \text{ cm}^{-1}.$$

The contribution to the spin-rotation splitting of the  $D$  state from states other than the  $C$  state is therefore  $+0.002 \text{ cm}^{-1}$ . Using second-order perturbation theory, Murphy (19) demonstrated that the spin-rotation constant,  $\gamma$ , will be characteristic of a given Rydberg series provided that quantum defects remain constant.<sup>2</sup> Figure 1, a plot of deperturbed values of  $\gamma$  versus effective principal quantum number, shows that once the perturbation by the  $C$  state is removed, the  $D$  state  $\gamma$  constant is similar in value to other members of the ' $s'$ '  $\Sigma$  series.

The  $D$  state vibrational constants determined by Fowler (10) were based on the location of observed  $P$ -branch heads. Fowler's constants were also based on incorrect

<sup>2</sup> Seemingly small deviations of observed principal quantum numbers,  $n^*$ , from their predicted values can produce enormous discrepancies between the observed and the calculated values of spin-rotation and  $\Lambda$ -doubling constants. This is because these constants are (to zero order) inversely proportional to  $\Delta E_{\Pi\Sigma}$  (see Eqs. (13)–(17)).  $\Delta E_{\Pi\Sigma}$  is proportional to  $\delta$ , the difference between the effective principal quantum numbers of the interacting  $\Pi$  and  $\Sigma$  states. Differences between observed and predicted values of  $n^*$  are largest at low energy, i.e., in the valence region.

$$\Delta E_{\Pi\Sigma} = R[(n_{\Sigma}^*)^{-2} - (n_{\Pi}^*)^{-2}] \cong 4R\delta(\bar{n}^{-3}); \quad \bar{n} \gg \delta$$

$$\bar{n} = \frac{1}{2}(n_{\Sigma}^* + n_{\Pi}^*), \quad \delta = \frac{1}{2}(n_{\Sigma}^* - n_{\Pi}^*), \quad R = 109\,737 \text{ cm}^{-1}.$$

The  $B^2\Sigma^+$  and  $E^2\Sigma^+$  spin-rotation constants are particularly affected by deviations of  $\delta$  from its large  $n^*$  limit. The  $B^2\Sigma^+$  state interacts primarily with  $A^2\Pi$  and  $E^2\Sigma^+$  with  $E'^2\Pi$ . The spin-rotation constant of the  $B$  and  $E$  states are "deperturbed" by multiplying the observed constant by  $\Delta E_{\Pi\Sigma}(\text{obs})/\Delta E_{\Pi\Sigma}(\text{calc})$ .  $\Delta E_{\Pi\Sigma}(\text{calc})$  is determined by assuming that quantum defects (and therefore  $\delta$ ) remain constant as Rydberg series are traced to low energy.

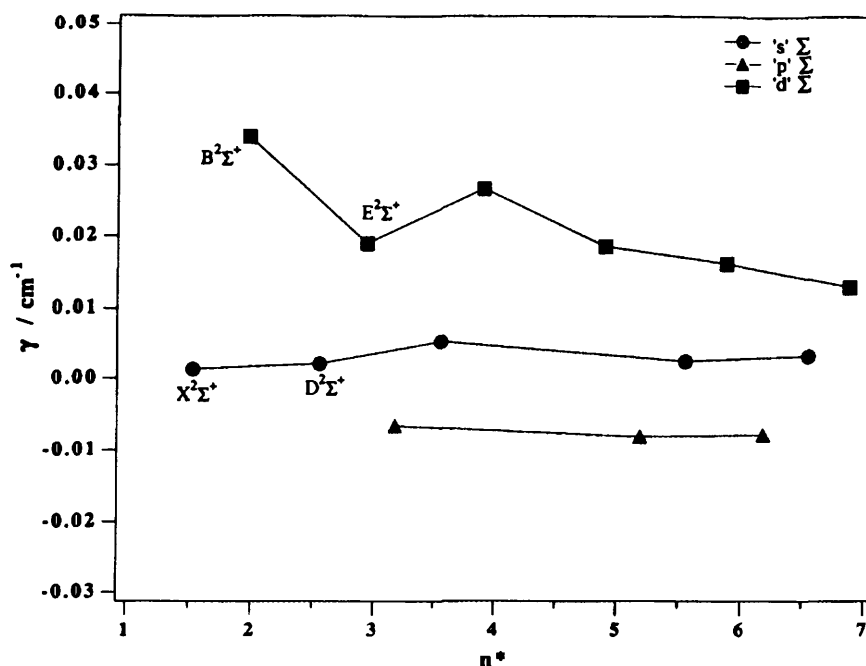


FIG. 1. Deperturbed spin-rotation constants of CaF <sup>2</sup>Σ<sup>+</sup> states.

upper vibrational level assignments. The *D* state vibrational quantum numbers listed in Fowler's paper should be uniformly increased by one. This has been pointed out previously by Ernst *et al.* (12) and Vergès *et al.* (13). We have converted Fowler's bandhead measurements to band origins (for both *C-X* and *D-X* progressions) and fit them, along with our more accurately determined term values for C<sup>2</sup>Π, *v* = 0, D<sup>2</sup>Σ<sup>+</sup>, *v* = 0, 1, and C<sup>2</sup>Π, *v* = 6 (Ref. 13), to the expression

$$\nu = T_e + \omega'_e(v' + \frac{1}{2}) - \omega_e x'_e(v' + \frac{1}{2})^2 - \omega''_e(v'' + \frac{1}{2}) + \omega_e x''_e(v'' + \frac{1}{2})^2. \quad (18)$$

The best-fit values are listed in Table III.

The calculated value of  $\Delta G_{1/2}$  for the D<sup>2</sup>Σ<sup>+</sup> state, 651.6(2) cm<sup>-1</sup>, is in excellent agreement with our observed value of 651.7(1) cm<sup>-1</sup>. The  $\alpha_e$  constant, as calculated by the Pekeris relation, is in good agreement with the observed difference in rotational constants between the *v* = 0 and *v* = 1 levels of the *D* state.

$$\alpha_{e,\text{calc}} = 6 \frac{B_e^2}{\omega_e} \left[ \left( \frac{\omega_e x_e}{B_e} \right)^{1/2} - 1 \right] = 0.00219(9) \text{ cm}^{-1}$$

$$\alpha_{e,\text{obs}} \cong B_0 - B_1 = 0.36453(2) - 0.36245(36) \text{ cm}^{-1} = 0.0021(4) \text{ cm}^{-1}. \quad (19)$$

Accurate molecular constants have now been determined for every CaF electronic state up to 35 650 cm<sup>-1</sup>. These constants have been archived in Ref. (3).

#### 4. DISCUSSION

We have determined accurate values of the C<sup>2</sup>Π and D<sup>2</sup>Σ<sup>+</sup> state molecular constants and provided an analysis of the observed Λ-doubling and spin-rotation splittings. Our

TABLE III  
Molecular Constants for  $X$ ,  $C$ , and  $D$  States (in  $\text{cm}^{-1}$ )<sup>a</sup>

	$C^2\Pi$	$D^2\Sigma^+$	$X^2\Sigma^+$
$T_e$	30269.21(15) <sup>b</sup>	30124.33(7)	0
$\omega_e$	481.78(40) <sup>b</sup>	657.33(15)	588.73(22) 588.87(32) <sup>c</sup>
$\omega_e x_e$	1.95(6) <sup>b</sup>	2.85(2)	2.81(3) 3.08(8) <sup>c</sup>
$B_e$	0.32439(1) <sup>d</sup>	0.3656(2) <sup>d</sup>	
$\alpha_e$	0.00205(2) <sup>d</sup>	0.0021(4) <sup>d</sup>	
$\alpha_e$ (Pekeris)	0.00190(5)	0.00219(1)	
$10^7 D_0$	5.84(5)	4.5(1)	
$10^7 D_e$ (Kratzer)	5.88(1)	4.52(1)	

<sup>a</sup> Uncertainties in parentheses represent two standard deviations.

<sup>b</sup> Fowler's (9) bandhead measurements were converted to band origins assuming  $A_v/\text{cm}^{-1} = 29.149 + 0.342(v + \frac{1}{2})$ , see Ref. (13).

<sup>c</sup> Ref. (14). Fixing the ground state vibrational constants to the values in Ref. (14) resulted in systematic errors in fitted C and D state band origins.

<sup>d</sup> Because  $B_v$  was determined for only two vibrational levels,  $B_e$  and  $\alpha_e$  are 100% correlated.

constants supersede the values reported by Fowler (10), Ernst *et al.* (12), and Vergès *et al.* (13). The inclusion of the  $p_D$  parameter in the Ref. (12) Hamiltonian lowers the authors' fitted value of the  $p$   $\Lambda$ -doubling constant. (The  $p_D$  parameter provides a  $J$ -dependent correction to  $p$ .) The Ref. (12) data were refitted with the  $p_D$  parameter set equal to zero and the lines nearest the avoided crossing were dropped from the fit. With this change in the Ref. (12) Hamiltonian and reduced Ref. (12) data set, the fitted value of the  $p$   $\Lambda$ -doubling constant converged to the value determined from a more complete data set fitted to the full  $C^2\Pi \sim D^2\Sigma^+$  effective Hamiltonian used in this work. To within the accuracy of the data, the effect of the  $p_D$  parameter can be entirely accounted for by the inclusion of off-diagonal matrix elements between the  $C^2\Pi$ ,  $v = 0$  and the  $D^2\Sigma^+$ ,  $v = 0$  vibronic levels.

The  $D$  state is the second member of the ' $s$ ' $\Sigma$  Rydberg series. Positive identification of the  $D$  state as the only  $^2\Sigma^+$  state in the region between 19 000 and 34 000  $\text{cm}^{-1}$  (i.e., between the  $B^2\Sigma^+$  and the  $E^2\Sigma^+$  states) allows us to conclude that the CaF  $\sigma$  Rydberg orbitals collapse smoothly into the molecular ion core as they are followed to low energy, i.e., as they become valence orbitals. To elucidate the transition from Rydberg to valence states, new ab initio calculations were performed for the first two members of the ' $s$ ' $\Sigma$  series, namely the  $X^2\Sigma^+$  and  $D^2\Sigma^+$  states. In comparison to the basis set used in Ref. (9), the Ca basis was expanded to include very diffuse  $s$  and  $d$  functions ( $\alpha_s = 0.005$ ,  $\alpha_d = 0.01$ ). The diffuse functions were included to better account for possible Rydberg  $\sim$  valence mixing. Using the improved basis set,  $T_e$  of the  $D^2\Sigma^+$  state was calculated to be 30 704  $\text{cm}^{-1}$ , which is in excellent agreement with the experimental value of 30 124  $\text{cm}^{-1}$ . Compared to Ref. (9),  $T_e$  decreased by about 2000  $\text{cm}^{-1}$ . This indicates that the inclusion of the Rydberg type  $s$  function is



very important for the description of the *D* state, i.e., the *D* state possesses partial Rydberg character. We conclude that the mixed character of the *D* state is the reason for the smooth transition from the Rydberg series to the valence states found for the 's' Σ series. This observation is consistent with the predictions of Berg *et al.*'s Rydberg state analysis (3) and Multichannel Quantum Defect Theory (7).

## ACKNOWLEDGMENTS

This work was partially supported by the National Science Foundation under Grant CHE91-20339. CMG thanks Lawrence Livermore National Laboratory for the loan of a pulsed Nd:YAG laser.

RECEIVED: April 27, 1993

## REFERENCES

1. S. RICE, H. MARTIN, AND R. W. FIELD, *J. Chem. Phys.* **82**, 5023-34 (1985).
2. J. E. MURPHY, J. M. BERG, A. J. MERER, N. HARRIS, AND R. W. FIELD, *Phys. Rev. Lett.* **65**, 1861-1864 (1990).
3. J. M. BERG, J. E. MURPHY, N. A. HARRIS, AND R. W. FIELD, *Phys. Rev. A*, in press (1993).
4. T. TORRING, W. ERNST, AND J. KÄNDLER, *J. Chem. Phys.* **90**, 4927-4932 (1989).
5. W. E. ERNST AND J. KÄNDLER, *Phys. Rev. A* **39**, 1575-1578 (1989).
6. N. A. HARRIS AND R. W. FIELD, *J. Chem. Phys.* **98**, 2642-2646 (1993).
7. N. A. HARRIS AND CH. JUNGEN, *Phys. Rev. Lett.*, **70**, 2549-2552 (1993).
8. P. BERNATH, Ph.D. Thesis, M.I.T. 1980.
9. P. BÜNDGEN, B. ENGELS, AND S. D. PEYERIMHOFF, *Chem. Phys. Lett.* **176**, 407-412 (1991).
10. C. A. FOWLER, *Phys. Rev.* **59**, 645-652 (1941).
11. A. J. KOTLAR, R. W. FIELD, J. I. STEINFELD, AND J. A. COXON, *J. Mol. Spectrosc.* **80**, 86-108 (1980).
12. W. E. ERNST, J. KÄNDLER, AND O. KNÜPPEL, *J. Mol. Spectrosc.* **153**, 81-90 (1992).
13. J. VERGÈS, C. EFFANTIN, A. BERNARD, A. TOPOUZKHANIAN, A. R. ALLOUCHE, J. D'INCAN, AND R. F. BARROW, *J. Phys. B*: **26**, 279-284 (1993).
14. P. BERNATH AND R. W. FIELD, *J. Mol. Spectrosc.* **82**, 339-347 (1980).
15. J. NAKAGAWA, P. J. DOMAILLE, T. C. STEIMLE, AND D. O. HARRIS, *J. Mol. Spectrosc.* **70**, 374-385 (1978).
16. M. DULICK, P. BERNATH, AND R. W. FIELD, *Can. J. Phys.* **58**, 703-712 (1980).
17. R. N. ZARE AND J. CASHION, unpublished (1963).
18. H. LEFEBVRE-BRION AND R. W. FIELD, "Perturbations in the Spectra of Diatomic Molecules," Academic Press, San Diego, 1986.
19. J. E. MURPHY, Ph.D. Thesis, M.I.T. 1992.